Available online at www.sciencedirect.com
SCIENCE DIRECT®
Mathematics and Computers in Simulation 65 (2004) 489–509
MATHEMATICS AND COMPUTERS IN SIMULATION
www.elsevier.com/locate/matcom

Applications of fully conservative schemes in nonlinear thermoelasticity: modelling shape memory materials

P. Matus [a], R.V.N. Melnik [b], L. Wang [b,*], I. Rybak [a]

[a] *Institute of Mathematics, National Academy of Sciences, Minsk 220072, Belarus*
[b] *Mads Clausen Institute, University of Southern Denmark, Grundtvigs Alle 150, DK-6400 Sønderborg, Denmark*

Abstract

In this paper, we consider a strongly coupled model of nonlinear thermoelasticity describing the dynamics of materials with shape memory. The model is not amenable to analytical treatments and the development, analysis, and applications of effective numerical approximations for this model is in the focus of the present paper. In particular, we discuss a recently proposed fully conservative difference scheme for the solution of the problem. We note that a standard energy inequality technique, applied to the analysis of convergence properties of the scheme, would lead to restrictive assumptions on the grid size and/or excessive smoothness assumptions on the unknown solution. We show how such assumptions can be removed to achieve unconditional convergence of the proposed scheme. Next, we apply the proposed scheme to the analysis of behaviour of a shape memory alloy rod. We demonstrate that the proposed approximation can describe a complete range of behaviour of the shape memory material, including quasiplastic, pseudoelastic, and almost elastic regimes. We discuss the influence of nonlinear effects in each of these regimes focusing on hysteresis effects.

Keywords: Dynamics; Hysteresis; Coupling; Shape memory effects; Fully conservative schemes; Unconditional convergence

1. Introduction

Upon the action of thermal, magnetic, electrical, hydrostatic and other fields, some specific materials can recover their original shape after being permanently deformed. In order to analyse the dynamics of these materials behaviour, we need to deal with multi-physics problems where interactions between two or more physical fields should be taken into account.

It has been shown experimentally that such metallic alloys as NiTi, NiAl, CuZnGa, CuZnAl, CuZn, CuAlNi, AuCuZn exhibit a hysteretic behavior and shape memory effects, subject to adequate thermo-mechanical conditions. The problem of the analysis of the behaviour of such materials can be formulated

* Corresponding author. Tel.: +45-6550-1660; fax: +45-6550-1660.
E-mail address: wanglinxiang@mci.sdu.dk (L. Wang).

0378-4754/$30.00 © 2004 IMACS. Published by Elsevier B.V. All rights reserved.
doi:10.1016/j.matcom.2004.01.012

mathematically on the basis of conservation law equations that incorporate a nonlinear coupling between mechanical and thermal fields.

A better understanding of the dynamics of shape memory alloy (SMA) materials is important for many areas of applications. These materials are an intrinsic part of the smart material and structure technology. They can directly transduce thermal energy into mechanical and vice versa, making them very attractive in micro-sensor and actuator applications. Other application areas include biomedicine, communication industries, robotics to name just a few. The analysis of shape memory materials has attracted a considerable attention of researchers, both experimentalists and theorists (e.g. [6,7,9,10,14,30,31,33]). Computational aspects of modelling shape memory materials have also been in the focus of a number of papers. One of the first papers in this field was [33] where the authors constructed and analysed a finite element approximation to a system describing phase transformations in a simple one-dimensional shape memory sample. In a series of papers, [30–32] the authors developed a generic procedure based on a low-dimensional reduction of the general three-dimensional systems describing the dynamics of shape memory materials. While at a theoretical level, the authors of [30–32] used effectively a blend between the centre manifold technique and computer algebra, the underlying numerical implementation was based on a differential–algebraic solver. However, there has been no systematic discussion in the literature devoted to fully conservative difference schemes for shape memory material applications. The construction of such schemes is a difficult task due to a strong nonlinear coupling of the associated system of partial differential equations. At the same time, the nonlinear coupling is essential in describing hysteresis effects, often accompanied by phase transformations. Since such phase transformations occur in SMA materials with a shearing motion of the crystal atoms without their large movements, they are often termed as “diffusionless” to reflect the fact that they occur practically instantaneously. The description of such “instantaneous” phase transformations and quantification of accompanied hysteresis effects is a very challenging computational task. The development and analysis of effective numerical approximations to coupled nonlinear models of thermoelasticity capable of describing these effects is the focus of the present paper.

In this paper, we consider a general model describing coupled thermomechanical wave interactions for the first order phase transitions. The model uses the Landau–Ginzburg–Devonshire representation of the free energy function, assuming that any isothermal equilibrium configuration of the lattice corresponds to a minimum (either local or global) of that function. In Section 2 we argue that such a model can be reduced to the Falk formulation in a number of practically important cases. Next, in Section 3 we discuss energy conservation properties of the model which we would like to preserve in our numerical approximation. The actual conservative scheme for the analysis of shape memory effects is discussed in Section 4 of the present paper. In Section 5, we formulate the problem for the error of our numerical approximation. We underline the main steps of the convergence analysis procedure and derive the main energy inequality in Section 6. Finally, in Section 7 we apply the scheme to the analysis of behaviour of a SMA rod and demonstrate that the proposed approximation can describe a complete range of behaviour of the shape memory material, including quasiplastic, pseudoelastic, and almost elastic regimes. We discuss the influence of nonlinear effects in each of these regimes focusing on hysteresis effects.

2. The model for shape memory material dynamics

We start our consideration from two conservation law equations, written for linear momentum and energy:

$$\begin{aligned}
&\rho\frac{\partial^2 u_i}{\partial t^2} = \nabla_x \cdot \vec{\sigma} + f_i, \quad i, j = 1, 2,\\
&\rho\frac{\partial e}{\partial t} - \vec{\sigma}^T : (\nabla \boldsymbol{v}) + \nabla \cdot \boldsymbol{q} = g,
\end{aligned} \tag{1}$$

where ρ is the density of the material, $\boldsymbol{u} = \{u_i\}|_{i=1,2}$ the displacement vector, $\boldsymbol{v}$ the velocity, $\vec{\sigma} = \{\sigma_{ij}\}$ the stress tensor, $\boldsymbol{q}$ the heat flux, e the internal energy, $\boldsymbol{f} = (f_1, f_2)^{\mathrm{T}}$ and g are mechanical and thermal loadings, respectively.

Given an appropriate model for the free energy function, the system (1) can describe coupled thermo-mechanical wave interactions during the first order phase transitions in a two dimensional SMA structure (e.g. [30,35,42]). Indeed, let ϕ be the free energy function of a thermomechanical system described by (1). Then, stress and the internal energy function are connected with ϕ by the following relationships

$$\vec{\sigma} = \rho\frac{\partial \phi}{\partial \vec{\eta}}, \quad e = \phi - \theta\frac{\partial \phi}{\partial \theta}, \tag{2}$$

where θ is the temperature, and the Cauchy–Lagrangian strain tensor $\vec{\eta}$ is given by its components as follows (with the repeated-index convention used)

$$\eta_{ij}(\boldsymbol{x}, t) = \left(\frac{\partial u_i(\boldsymbol{x}, t)}{\partial x_j} + \frac{\partial u_j(\boldsymbol{x}, t)}{\partial x_i}\right)\Big/ 2, \quad i, j = 1, 2, \tag{3}$$

where $\boldsymbol{x}$ is the coordinates of a material point in the domain of interest.

Following [42] (and references therein), we note that for the square-to-rectangular transformations [20,21] we can represent the free energy function of our thermomechanical system by using the Landau form F_{L}

$$\begin{aligned}
&\phi = -c_v\theta \ln \theta + \tfrac{1}{2}a_1 e_1^2 + \tfrac{1}{2}a_3 e_3^2 + F_{\mathrm{L}},\\
&F_{\mathrm{L}} = \tfrac{1}{2}a_2(\theta - \theta_0)e_2^2 - \tfrac{1}{4}a_4 e_2^4 + \tfrac{1}{6}a_6 e_2^6,
\end{aligned} \tag{4}$$

where c_v is the specific heat constant, θ_0 is the martensite transition temperature, a_i, $i = 1$–$4, 6$ are the material-specific coefficients, and

$$e_1 = \frac{(\eta_{11} + \eta_{22})}{\sqrt{2}}, \quad e_2 = \frac{(\eta_{11} - \eta_{22})}{\sqrt{2}}, \quad e_3 = \frac{(\eta_{12} + \eta_{21})}{2} \tag{5}$$

are dilatational, deviatoric, and shear components of strain, respectively. Then, combining (2)–(5) and (1), we obtain the following model

$$\begin{aligned}
&\frac{\partial^2 u_1}{\partial t^2} = \frac{\sqrt{2}}{2}\frac{\partial}{\partial x}(a_1 e_1 + a_2(\theta - \theta_0)e_2 - a_4 e_2^3 + a_6 e_2^5) + \frac{\partial}{\partial y}\left(\frac{1}{2}a_3 e_3\right) + f_1,\\
&\frac{\partial^2 u_2}{\partial t^2} = \frac{\partial}{\partial x}\left(\frac{1}{2}a_3 e_3\right) + \frac{\sqrt{2}}{2}\frac{\partial}{\partial y}(a_1 e_1 - a_2(\theta - \theta_0)e_2 + e_4 e_2^3 - a_6 e_2^5) + f_2,\\
&c_v\frac{\partial \theta}{\partial t} = k\left(\frac{\partial^2 \theta}{\partial x^2} + \frac{\partial^2 \theta}{\partial y^2}\right) + \frac{\sqrt{2}}{2}a_2\theta e_2\frac{\partial e_2}{\partial t} + g.
\end{aligned} \tag{6}$$

We consider a situation where the deformation of a 2D SMA sample along x_1 direction substantially exceeds the deformation in the other direction, so that the deformation along x_2 direction can be neglected and the sample can be treated as a SMA rod. In this case, $\partial u_2/\partial x_2 = 0$, $\partial u_2/\partial x_1 = 0$, $\partial u_1/\partial x_2 = 0$, and system (6) is reduced to

$$\begin{aligned} \frac{\partial^2 u_1}{\partial t^2} &= \frac{\partial}{\partial x}\left(\frac{\sqrt{2}}{2}(a_1\epsilon + a_2(\theta-\theta_0)\epsilon - a_4\epsilon^3 + a_6\epsilon^5)\right) + f_1, \\ c_v\frac{\partial\theta}{\partial t} &= k\left(\frac{\partial^2\theta}{\partial x^2}\right) + \frac{\sqrt{2}}{2}a_2\theta\epsilon\frac{\partial\epsilon}{\partial t} + g. \end{aligned} \tag{7}$$

It is straightforward to see that system (7) can be re-cast in the Falk form with $\theta_1 = \theta_0 - a_1/a_2$:

$$\begin{aligned} \rho\frac{\partial^2 u}{\partial t^2} &= \frac{\partial}{\partial x}\left(k_1(\theta-\theta_1)\frac{\partial u}{\partial x} - k_2\left(\frac{\partial u}{\partial x}\right)^3 + k_3\left(\frac{\partial u}{\partial x}\right)^5\right) + F, \\ c_v\frac{\partial\theta}{\partial t} &= k\frac{\partial^2\theta}{\partial x^2} + k_1\theta\frac{\partial u}{\partial x}\frac{\partial v}{\partial x} + G, \end{aligned} \tag{8}$$

where k_1–k_3 are re-normalised material-specific constants, and F and G are distributed mechanical and thermal loadings. As before, u is the displacement of the rod, ρ is the density of the material, k is the thermal conductivity, c_v is the specific heat constant, θ_1 is a positive constant that characterises a critical temperature of the material.

System (8) is completed by appropriate initial and boundary conditions and has to be solved with respect to (u, θ) in the spatial-temporal region $\Omega = \{(x, t) : 0 \le x \le L, 0 \le t \le T_f\}$, where L is the length of the shape memory rod and T_f is the limiting time moment.

Since the shape memory material can be in a high temperature phase (austenite) as well as in a low temperature phase (martensite), at the computational level one faces a fairly complex task of dealing with different equilibrium configurations of the metallic lattice simultaneously. Therefore, it is important to preserve intrinsic properties of model (8) at the discrete level.

3. Establishing properties of the model to be inherited by the difference scheme

The success of modelling is often dependent on how well the invariant properties of the original differential model are reflected in the numerical approximation. Difference numerical approximations for which discrete analogues of conservation laws are satisfied are known as conservative (e.g. [38]). Conservative numerical schemes play a fundamental role in applications, and their development for coupled nonlinear problems constitutes an important task in applied numerical mathematics. Such schemes preserve fundamental properties of the continuous model at the discrete level and allow us to carry out computations on coarse grids with minimal computational expenses. The fundamentals of what is now known as the energy method stem from the seminal work of Courant et al. [11]. However, as it was pointed out in [15], in that work and in a series of other works that followed in the subsequent decades a major emphasis was often given to stability properties of numerical approximations rather than to the energy conservation property itself.

A turning point in this development was work [39] where conservative difference schemes were constructed for a class of problems with discontinuous coefficients. A natural extension of that early work was the development of the concept of full conservativeness. The full conservativeness requires not only discrete analogues of conservation laws to be fulfilled, but also additional relationships that express a balance of different types of energy [36]. Conservative and fully conservative schemes have been developed in a number of application areas, gas-, magneto-, and hydro-dynamic applications to mention just a few (e.g. [18,36] and references therein). Several different methodologies have been developed in the literature for the construction of such schemes, in particular those based on the integro-interpolational, variational, and projection methodologies (e.g. [8,17,39] and references therein). Those results have created a foundation for further construction, development, and applications of conservative difference schemes in a range of problem areas, including linear and nonlinear models for deformable elastic media [40,41]. Recent re-discovery of these methodologies (e.g. [16,25]) has led to their further development and applications to complex nonlinear problems, including those involving phase transition problems (see, for example, [16] where conservative schemes have been applied to the Cahn-Hilliard model).

In the remainder of this section, we aim at establishing, under certain conditions, the conservation law of the total energy of the system described by models like (8). One of the difficulties in the numerical solution of system (8) lies with the fact that the stress–strain dependency here is a nonmonotone function. In [30–32], an efficient numerical methodology was developed based on a reduction of the original model to a system of differential–algebraic equations. The main differential variables of the system were u, v, and θ, while the equation for stress was handled as a differential–algebraic equation. In what follows, a different idea is developed. We will treat the stress–strain dependency as a purely algebraic equation by introducing ϵ, v, and θ as differential variables, in which case s can be written as an algebraic equation in terms of ϵ. We have:

$$\epsilon = \frac{\partial u}{\partial x}, \quad v = \frac{\partial u}{\partial t}, \quad s = k_1(\theta - \theta_1)\epsilon - k_2\epsilon^3 + k_3\epsilon^5, \tag{9}$$

where s is the stress and the last relationship between stress and strain functions in the one-dimensional case follows directly from the Falk representation of the free energy and the first relationship (2). Hence, problem (8) can be recast as:

$$\begin{aligned} &\frac{\partial \epsilon}{\partial t} = \frac{\partial v}{\partial x}, \quad \rho\frac{\partial v}{\partial t} = \frac{\partial s}{\partial x} + F, \\ &C_v\frac{\partial \theta}{\partial t} = k\frac{\partial^2 \theta}{\partial^2 x} + k_1\theta\epsilon\frac{\partial v}{\partial x} + G, \quad s = k_1(\theta - \theta_1)\epsilon - k_2\epsilon^3 + k_3\epsilon^5, \end{aligned} \tag{10}$$

where, as an example, we choose the following initial and boundary conditions

$$\begin{aligned} &\epsilon(x,0) = \frac{\partial u^0(x)}{\partial x}, \quad v(x,0) = u^1(x), \quad \theta(x,0) = \theta^0(x), \\ &s(0,t) = \bar{s}_1(t), \quad s(L,t) = \bar{s}_2(t), \quad \frac{\partial \theta}{\partial x}(0,t) = \bar{\theta}_1(t), \quad \frac{\partial \theta}{\partial x}(L,t) = \bar{\theta}_2(t). \end{aligned} \tag{11}$$

Following [29], we obtain that in the absence of distributed loadings ($F = G = 0$), systems like (10)–(11) are characterised by the conservation law of the total energy which can be written in the following form

$$\mathcal{E}(t) = \mathcal{E}(0), \tag{12}$$

where the full energy of the system is understood as

$$\mathcal{E}(t) = \rho||v||^2 + \left(2C_v\theta - k_1\theta_1\epsilon^2 - \frac{k_2}{2}\epsilon^4 + \frac{k_3}{3}\epsilon^6, 1\right) - \int_0^t \left(2k\frac{\partial\theta}{\partial x} + sv\right)|_0^t \mathrm{d}t \tag{13}$$

with scalar products taken in space L_2. The result (12) is obtained by multiplying the second equation in (10) by $2v$, integrating the result over the entire domain Ω and performing integration by parts, accounting for boundary conditions (11).

Now, we would like to preserve the property (12) on the grid. To achieve this, we employ an idea for the construction of fully conservative schemes based on the integro-interpolational methodology [38] with the following modification. In addition to the interpolation of the sought-for solution with respect to independent variables, we perform the Steklov averaging of nonlinear terms. This idea has been applied successfully before in in the context of constructing conservative numerical schemes for several classes of nonlinear problems of mathematical physics (e.g. [2–4] and references therein).

4. Conservative scheme for the analysis of shape memory effects

Numerical schemes that have a minimal sensitivity to the regularity of the grid are important in many areas of applications (e.g. [1,28,29]). For the problems like ours, it is important to be able to compute the solution on relatively coarse grids for large time intervals. This can be achieved with conservative numerical schemes.

In the closed interval $[0, L]$, we define the space grid with integer points x_i and flux points $\bar{x}_i$ as $x_i = ih, i = 0, 1, 2, \ldots, N$, and $\bar{x}_i = (i + 1/2)h, i = 0, 1, 2, \ldots, N - 1$, respectively, where N is the number of grid points satisfying equality $hN = L$. The set of these points will be denoted by $\bar{\omega}_h$. Strain ϵ, temperature θ and stress s are approximated in the integer grid points x_i and are denoted here by ϵ_i, θ_i and s_i, respectively, while velocity v is approximated in the flux points $\bar{x}_i$ and is denoted here by $v_{i+1/2}$ (or by $\bar{v}$ where appropriate). We note that the scheme described below is a second order scheme obtained on the minimal stencil [29]. Nonlinear terms (in particular, ϵ^4 and ϵ^6) are averaged here in the Steklov sense, so that for nonlinear function $f(\xi)$, averaged in the the interval $[\epsilon, \bar{\epsilon}]$, we have

$$g(\epsilon, \bar{\epsilon}) = \frac{1}{\bar{\epsilon} - \epsilon}\int_{\epsilon}^{\bar{\epsilon}} f(\eta)\,\mathrm{d}\eta, \quad \epsilon = \epsilon^n = \epsilon(t_n), \quad \bar{\epsilon} = \epsilon^{n+1} = \epsilon(t_{n+1}). \tag{14}$$

This averaging procedure and its development in the context of several classes of nonlinear problems of mathematical physics goes back to works [2–4]. In our context, the procedure allows us to construct a scheme for which a discrete analogue of (12) is fulfilled.

The discretization in time is carried out with time step τ, so that the scheme constructed has the following form

$$\begin{aligned}
&\frac{\epsilon_i^{n+1}-\epsilon_i^n}{\tau}=\frac{v_{i+1/2}^{\sigma_1}-v_{i-1/2}^{\sigma_1}}{h},\quad i=1,2,\dots,N-1,\\
&\rho\frac{v_{i+1/2}^{n+1}-v_{i+1/2}^n}{\tau}=\frac{s_{i+1}^{n+1}-s_i^{n+1}}{h},\quad i=0,1,2,\dots,N-1,\\
&C_v\frac{\theta_i^{n+1}-\theta_i^n}{\tau}=k\frac{\theta_{i+1}^{\sigma_3}-2\theta_i^{\sigma_3}+\theta_{i-1}^{\sigma_3}}{h^2}+k_1\theta_i^{\sigma_3}\epsilon_i^{\sigma_2}\frac{v_{i+1/2}^{\sigma_1}-v_{i-1/2}^{\sigma_1}}{h},\quad i=1,2,\dots,N-1,\\
&s_i^{n+1}=k_1(\theta_i^{\sigma_3}-\theta_1)\epsilon_i^{\sigma_2}-\frac{k_2}{4}g_1(\epsilon_i^n,\epsilon_i^{n+1})+\frac{k_3}{6}g_2(\epsilon_i^n,\epsilon_i^{n+1}),
\end{aligned}\tag{15}$$

where

$$g_1(\epsilon,\bar\epsilon)=\frac{\bar\epsilon^4-\epsilon^4}{\bar\epsilon-\epsilon}=\sum_{k=0}^{3}\bar\epsilon^{3-k}\epsilon^k,\quad g_2(\epsilon,\bar\epsilon)=\frac{\bar\epsilon^6-\epsilon^6}{\bar\epsilon-\epsilon}=\sum_{k=0}^{5}\bar\epsilon^{5-k}\epsilon^k\tag{16}$$

and, as usual, the discrete function with weight σ is defined by

$$y^\sigma=\sigma y^{n+1}+(1-\sigma)y^n,\quad 0\le\sigma\le 1.\tag{17}$$

Discrete problem (15)–(17) is supplemented by the initial

$$\epsilon_i^0=\frac{\partial u^0}{\partial x}(x_i),\quad v_{i+1/2}^0=u^1(\bar x_i),\quad \theta_i^0=\theta^0(x_i),\tag{18}$$

and boundary

$$\begin{aligned}
&s_0^{n+1}=\bar s_1(t_{n+1}),\quad s_N^{n+1}=\bar s_2(t_{n+1}),\\
&\frac{\theta_1^{\sigma_3}-\theta_0^{\sigma_3}}{h}-\frac{h}{2}\left(\frac{C_v}{k}\frac{\theta_0^{n+1}-\theta_0^n}{\tau}-\frac{k_0}{k}\theta_0^{\sigma_3}\epsilon_0^{\sigma_2}\frac{\epsilon_0^{n+1}-\epsilon_0^n}{\tau}\right)=\bar\theta_1^{\sigma_3},\\
&\frac{\theta_N^{\sigma_3}-\theta_{N-1}^{\sigma_3}}{h}+\frac{h}{2}\left(\frac{C_v}{k}\frac{\theta_N^{n+1}-\theta_N^n}{\tau}-\frac{k_0}{k}\theta_N^{\sigma_3}\epsilon_N^{\sigma_2}\frac{\epsilon_N^{n+1}-\epsilon_N^n}{\tau}\right)=\bar\theta_2^{\sigma_3},
\end{aligned}\tag{19}$$

conditions. Difference scheme (15)–(19) approximates the differential problem (10)–(11) with $\mathbb{O}(h^2+(\sigma_k-0.5)\tau+\tau^2)$ order in space-time. In obtaining approximations (19) for the thermal field, the standard technique of approximation of the third-kind boundary conditions with second order was applied (e.g. [38]). For simplicity of the analysis, we will replace the constant values $\theta_0^{(\sigma_3)}$ and $\theta_N^{(\sigma_3)}$ in (19) by $\theta_1=\text{const}$. In practice, this may reduce the order of the error of approximation in space by one. However, conservative properties of the scheme will be preserved even in this case.

The above difference scheme satisfies a discrete analogue of energy conservation (12). Recall that the main result of [29], stated there without proof, is the following energy equality:

$$\mathbb{E}_{1h}(t+\tau) + \sum_{\tau\in\omega_\tau} \mathbb{E}_{2h}(t) - 2\sum_{\tau\in\omega_\tau} \tau\gamma_h(t) = \mathbb{E}_{1h}(0), \quad t \in \omega_\tau, \tag{20}$$

where discrete analogues of the energy norms $\mathbb{E}_{1h}$, $\mathbb{E}_{2h}$, and $\gamma_h(t)$ are defined as follows

$$\mathbb{E}_{1h} = \rho|[\bar{v}|| + 2C_v[\theta, 1] - k_1\theta_1|[\epsilon]|^2 - \tfrac{k_2}{2}||\epsilon^2||^2 + \tfrac{k_3}{2}||\epsilon^3||^2, \tag{21}$$

$$\mathbb{E}_{2h} = 2\tau^2\rho(\sigma_1 - 0.5)|[\bar{v}_t||^2 + 2k_1\theta_1\tau^2(\sigma_2 - 0.5)|[\epsilon_t]|^2, \tag{22}$$

$$\gamma_h(t+\tau) = k\theta_2^{(\sigma_3)} + \hat{s}_N\bar{v}_{N-1}^{(\sigma_1)} - k\theta_1^{(\sigma_3)} - \hat{s}_0\bar{v}_0^{(\sigma_1)}. \tag{23}$$

In (20)–(23), we use standard notations of theory of difference schemes [38]. In particular, by $y_{\bar{x}}$ and y_x we denote left and right first difference derivatives of y wrt x, while $\hat{y} \equiv y(t+\tau)$ whenever $y \equiv y(t)$, $\tau \in \omega_\tau \equiv \{t_n = n\tau, n = 1, \ldots, N_0 - 1, \tau N_0 = T_f\}$. The discrete L_2 norms are defined in a usual manner

$$||u|| = \sqrt{(u,u)}, (u,v) = \sum_{x\in\omega_h} huv, \quad ||u]| = \sqrt{(u,u]}, (u,v] = \sum_{x\in\omega_h^+} huv, \tag{24}$$

where $\omega_h^+ = \{x_i = ih, i = 1, \ldots, N\}$ and norm $|[u||$ is defined analogously to (24).

To show that the discrete analogue of energy conservation (20) is satisfied, similar to the continuous case we multiply both parts of the second equation in (15) by $2v^{\sigma_1}$ and perform the summation over $i = 0, 1, \ldots, N-1$. First, we note that

$$[\bar{v}, s_{\bar{x}}) = -(s, \bar{v}_{\bar{x}}] + s_N\bar{v}_{N-1} - \bar{v}_0 s_0 \tag{25}$$

is valid for arbitrary grid functions $\bar{v} \equiv v(x + h/2)$ and $s(x)$ whenever $x \in \omega_h$. The above equality (a discrete analogue of Green's formula) follows directly from the difference summation by parts

$$\sum_{i=1}^{N-2} h\bar{v}_i s_{x,i} = -\sum_{i=1}^{N-1} h\bar{v}_{\bar{x},i}s_i + s_{N-1}\bar{v}_{N-1} - \bar{v}_0 s_1. \tag{26}$$

Using (25) and that $y^{(\sigma)} = y^{(0.5)} + \tau(\sigma - 0.5)y_t \; \forall\sigma \in [0,1]$, we arrive at the following result:

$$\rho(|[\bar{v}||^2)_t + 2\tau(\sigma_1 - 0.5)|[\bar{v}_t||^2) + 2(\hat{s}, \bar{v}_{\bar{x}}^{(\sigma_1)}) - 2(\hat{s}_N\bar{v}_{N-1}^{(\sigma_1)} - \hat{s}_0\bar{v}_0^{(\sigma_1)}) = 0. \tag{27}$$

The third term in the left hand side of (27) needs to be transformed. This is achieved in several steps. Firstly, we use the first and the last equations of (15) to rewrite this term as follows:

$$\begin{aligned} 2(\hat{s}, \bar{v}_{\bar{x}}^{(\sigma_1)}) &= 2\left(k_1(\theta^{(\sigma_3)} - \theta_1)\epsilon^{(\sigma_2)} - \frac{k_2}{4}\frac{\hat{\epsilon}^4 - \epsilon^4}{\hat{\epsilon} - \epsilon} + \frac{k_3}{6}\frac{\hat{\epsilon}^6 - \epsilon^6}{\hat{\epsilon} - \epsilon}, \frac{\hat{\epsilon} - \epsilon}{\tau}\right) \\ &= 2(k_1\theta^{(\sigma_3)}\epsilon^{(\sigma_2)}\bar{v}_{\bar{x}}^{(\sigma_1)}, 1) - k_1\theta_1((||\epsilon||^2)_t + 2\tau(\sigma_2 - 0.5)||\epsilon_t||^2)\left(-\frac{k_2}{2}||\epsilon^2||^2 + \frac{k_3}{3}||\epsilon^3||^2\right)_t. \end{aligned} \tag{28}$$

This still requires further transformations due to the presence of term $(k_1\theta^{(\sigma_3)}\epsilon^{(\sigma_2)}\bar{v}_{\bar{x}}^{(\sigma_1)}, 1)$ which can be re-written by taking into account (19) as follows:

$$\begin{aligned}(k_1\theta^{(\sigma_3)}\epsilon^{(\sigma_2)}\bar{v}_{\bar{x}}^{(\sigma_1)}, 1) &= 2(C_v\theta_t - k\theta_{\bar{x}x}^{(\sigma_3)}, 1) = (2C_v\theta, 1)_t - 2k(\theta_{\bar{x},N}^{(\sigma_3)} - \theta_{\bar{x},0}^{(\sigma_3)}) \\ &= [2C_v\theta, 1]_t - \tfrac{h}{2}((k_1\theta_1, (\epsilon_0^2)_t + 2\tau(\sigma_2 - 0.5)\epsilon_{t,0}^2) \\ &\quad + (k_1\theta_1, (\epsilon_N^2)_t + 2\tau(\sigma_2 - 0.5)\epsilon_{t,N}^2)) - 2k(\theta_2^{(\sigma_3)} - \theta_2^{(\sigma_1)}),\end{aligned} \tag{29}$$

where, as usual, we denote by $y_{\bar{x}x}$ the second central difference derivative of function y wrt x (e.g. [38]). In obtaining (29), we have replaced for simplicity the values of $\theta_0^{\sigma_3}$ and $\theta_N^{\sigma_3}$ by a constant denoted by θ_1. Hence, the actual boundary conditions used in obtaining a discrete analogue of the energy conservation can be written as follows (see comments after (19)):

$$\begin{aligned}\theta_{x,0}^{(\sigma_3)} - \frac{h}{2}\left(\frac{C_v}{k}\theta_{t,0} - \frac{k_1\theta_1}{k}\epsilon_0^{(\sigma_2)}\epsilon_{t,0}\right) &= \bar{\theta}_1^{(\sigma_3)} \\ \theta_{x,N}^{(\sigma_3)} + \frac{h}{2}\left(\frac{C_v}{k}\theta_{t,N} - \frac{k_1\theta_1}{k}\epsilon_N^{(\sigma_2)}\epsilon_{t,N}\right) &= \bar{\theta}_2^{(\sigma_3)}.\end{aligned} \tag{30}$$

With this in mind, we substitute (29) into (28) and use the result in (27) to get

$$\mathbb{E}_{1h}(t+\tau) + \mathbb{E}_{2h}(t) - 2\tau(k\theta_2^{(\sigma_3)} + \hat{s}_N\bar{v}_{N-1}^{(\sigma_1)} - k\theta_1^{(\sigma_3)} - \hat{s}_0\bar{v}_0^{(\sigma_1)}) = \mathbb{E}_{1h}(t). \tag{31}$$

Performing summation of (31) over all $t \in \omega_\tau$, we obtain

$$\mathbb{E}_{1h}(t+\tau) + \sum_{t\in\omega_\tau}\mathbb{E}_{2h}(t) - 2\tau\sum_{t\in\omega_\tau}(k\theta_2^{(\sigma_3)} + \hat{s}_N\bar{v}_{N-1}^{(\sigma_1)} - k\theta_1^{(\sigma_3)} - \hat{s}_0\bar{v}_0^{(\sigma_1)}) = \mathbb{E}_{1h}(0) \tag{32}$$

which, taking into account (21)–(22), coincides with (20).

By analysing (32), we come to the conclusion that the derived scheme is fully conservative if $\Delta\mathbb{E} \equiv \sum_{t\in\omega_\tau}\mathbb{E}_{2h}(t) = 0$ [29]. This energy disbalance term will be zero if we choose $\sigma_1 = \sigma_2 = 0.5$ which in this case will be necessary conditions for full conservativeness of the constructed scheme. Furthermore, from a physical point of view the values of θ should be positive. This is achieved for the purely implicit scheme with $\sigma_3 = 1$. In this case, we finally arrive at the following discrete analogue of energy conservation

$$\mathbb{E}_h(t) = \mathbb{E}_h(0), \tag{33}$$

where we set $\mathbb{E}_h(t) = \mathbb{E}_{1h}(t) - 2\tau\sum_{t\in\omega_\tau}\gamma_h(t)$. As we have already mentioned in [29], an a priori estimate for the discrete problem with homogeneous boundary conditions (30) follows from (33) in the specified combined discrete norm under the above choice of weight parameters.

We conclude this section with several remarks concerning concepts of conservativeness and full conservativeness. There are several different definitions of conservativeness of difference schemes and their equivalence was established in [34]. It seems that the notion of full conservativeness is used sometimes in a wider sense than it was originally proposed in [36]. For example, in the CFD community all schemes that discretely conserve mass, momentum, and kinetic energy (in the inviscid limit) are often called fully conservative (see [1,19] and references therein). Moreover, many of the ideas proposed recently seem to be developed independently of much earlier works performed for gas- and hydro-dynamic applications (e.g. [17,18]), although conceptual basis and methodologies for constructing fully conservative schemes in these cases are quite similar.

With growing areas of applications of nonlinear models of mathematical physics the interest to fully conservative numerical approximations continues to increase [37]. Furthermore, over the last several decades there have been continuing efforts in developing a unified framework for constructing high-order schemes for conservative/dissipative systems (e.g. [25] and references therein) and in extending Noether theorem to a large class of difference schemes that possess an equivalent variational formulations (e.g. [12,23]).

5. Analysis of the discrete model

Before proceeding to numerical experiments with (15)–(19), we shall highlight the main steps of the convergence analysis of the proposed scheme.

Classical approaches to the analysis of stability and convergence of numerical approximations for nonlinear problems of mathematical physics rely typically on certain global assumptions about the coefficients of the models which, in the case of nonlinear problems, depend on the solution itself. In particular, we often need to satisfy certain constraints such as boundness of the derivatives with respect to the solution for all set of possible exact solutions, e.g. the solution may be considered in the entire $\mathbb{R}$ [28]. Such problems, known as problems with bounded nonlinearities, do not include many problems of practical interests, where coefficients of the model may retain their properties only in a small neighbourhood of variation of the exact solution. The problems considered in the present paper belong to the latter class. One of the consequences of unbounded nonlinearities is that the problem for the error of approximation becomes nonlinear which complicates the analysis substantially [28]. One way to analyse convergence properties of numerical schemes for these types of problems is to use a well-known methodology based on energy inequalities. This methodology has recently been applied in the context of several classes of nonlinear problems (e.g. [1,15,16]). However, a conventional application of the method to problems with unbounded nonlinearities leads to restrictive assumptions on the grid size and/or excessive smoothness assumptions on the unknown solution. Such assumptions are very undesirable, in particular in the problems like ours where the ability of computing the solution even on coarse grids for large time intervals is essential. Indeed, unconditionally convergent numerical approximations is a desirable feature of computational algorithms and such algorithms have already been discussed in the context of several application areas (e.g. [5,22,24]).

A methodology for analysing unconditionally convergent algorithms for a class of models with unbounded nonlinearities was proposed in [27]. The methodology was based on a combination of the so-called ν-method (e.g. [2]) and the methodology developed in [26]. In what follows, we employ this methodology in the analysis of the proposed difference scheme. The basic idea behind this generalised ν-methodology consists of proving unconditional convergence of the scheme in the uniform norm by considering separately situations of $\tau \le \alpha_0 h$ and $\tau > \alpha_0 h$ (where, as before, τ and h are time and space discretisation steps, and α_0 is a given constant). Each of these two cases requires a choice of a specific norm in which it is possible to establish a priori estimates for the problem solution, and which then can be improved at the next stage of the procedure (e.g. [26]).

As the first step of our analysis, we derive in this section a problem for the approximation error for one of the schemes from class (15)–(19). As an example, we consider the following scheme which we write in the index-free notation (e.g. [38]):

$$(\epsilon_h)_t = (\bar{v}_h)_{\bar{x}}^{(0.5)}, \quad \rho(\bar{v}_h)_t = (\hat{s}_h)_x, \quad \hat{s}_h = k_1(\hat{\theta}_h - \theta_1)\hat{\epsilon}_h - k_2\hat{\epsilon}_h^3 + k_3\hat{\epsilon}_h^5,$$
$$c_v(\theta_h)_t = k(\hat{\theta}_h)_{\bar{x}x} + k_1\hat{\theta}_h\hat{\epsilon}_h(\epsilon_h)_t, \tag{34}$$

where $y = (\epsilon_h, \bar{v}_h, \theta_h)$ is a vector of the approximate solution (a vector of discrete functions of the grid size), obtained with scheme (34). When it does not lead to ambiguity, we use the bar to indicate the value calculated at the flux point (that is $\bar{v}_h = v_h(x_{i+1/2}, t_n)$), and the exact solution calculated at the same grid point will be denoted by $u = (\epsilon, \bar{v}, \theta)$. We are in a position to introduce the error of approximation as $z = y - u = (\Delta\epsilon, \Delta v, \Delta\theta)$, where

$$\Delta\epsilon = \epsilon_h - \epsilon, \quad \Delta v = \bar{v}_h - \bar{v}, \quad \Delta\theta = \theta_h - \theta. \tag{35}$$

We substitute functions ϵ_h, $\bar{v}_h$, and θ_h, found from (35), into the scheme (34). We have immediately that

$$\Delta\epsilon_t = \Delta v_{\bar{x}}^{(0.5)} + \psi_1^{(0.5)}, \quad \rho\Delta v_t = \Delta\hat{s}_x + \hat{\psi}_2, \tag{36}$$

where

$$\psi_1^{(0.5)} = -\epsilon_t + \bar{v}_{\bar{x}}^{(0.5)} = \mathbb{O}(h^2 + \tau^2), \quad \hat{\psi}_2 = -\rho\bar{v}_t + \hat{s}_x = \mathbb{O}(h^2 + \tau). \tag{37}$$

After some tedious transformations we obtain the following equation for the error of approximation $\Delta\theta$:

$$\begin{aligned} c_v\Delta\theta_t = {} & k\Delta\hat{\theta}_{\bar{x}x} + k_1\hat{\epsilon}\epsilon_t\Delta\hat{\theta} + k_1\hat{\theta}\epsilon_t\Delta\hat{\epsilon} + k_1\hat{\theta}\hat{\epsilon}\Delta\epsilon_t + k_1\hat{\theta}\Delta\hat{\epsilon}\Delta\epsilon_t \\ & + k_1\hat{\epsilon}\Delta\hat{\theta}\Delta\epsilon_t + k_1\epsilon_t\Delta\hat{\theta}\Delta\hat{\epsilon} + k_1\Delta\hat{\theta}\Delta\hat{\epsilon}\Delta\epsilon_t + \hat{\psi}_3, \end{aligned} \tag{38}$$

where

$$\hat{\psi}_3 = -c_v\theta_t + k\hat{\theta}_{\bar{x}x} + k_1\hat{\theta}\hat{\epsilon}\epsilon_t = \mathbb{O}(h^2 + \tau). \tag{39}$$

Initial and boundary conditions of the problem for the error approximation are homogeneous

$$\Delta\epsilon^0 = \Delta\theta^0 = \Delta v^0 = 0, \tag{40}$$

$$\Delta\epsilon_0^{n+1} = \Delta\epsilon_0^{n+1} = 0, \quad \Delta\theta_0^{n+1} = \Delta\theta_0^{n+1} = 0. \tag{41}$$

Hence, the problem for the error of approximation of our scheme (34) is completely defined by (36)–(41).

6. Energy inequalities and main steps of the convergence analysis

The analysis of convergence of solutions of difference schemes for nonlinear problems of mathematical physics is an important and difficult task. The standard ν-method (e.g. [2,26]) works well for a wide class of nonlinear problems, but in its implementation requires quite restrictive assumptions on the grid size (typically such as $\tau = h^\kappa$, $\kappa > 1$, e.g. [13,3] and references therein). Since conservative schemes are known for their robustness even on coarse grids, it is desirable to remove such assumptions when the convergence of the scheme is analysed. One way to do that is to use an assumption of the increased solution smoothness [16]. However, in the problems like ours it is not an option since we have to deal with steep gradients in the solution (e.g. [30,42]). A two-stage methodology that does not require excessive smoothness assumptions has been originally proposed in [26]. It rests on the analysis of the difference solution in discrete norms L_2 and W_2^1. More precisely, first we analyse the difference solution in the grid norm L_2 and C under the condition $\tau \le \alpha_0 h$ with given $\alpha_0 = \text{const} > 0$ (e.g. $\alpha_0 = 1$), and then we carry out the analysis of the solution in the discrete norm W_2^1 in the case $\tau \ge \alpha_0 h$. Combining these two results yields to unconditional convergence of the difference solution in the uniform norm. The success

of the methodology ultimately rests on the embedding theorems. Indeed, if one analyses the difference solution in L_2, the assumption $\tau \le \alpha_0 h$ is a consequence of the embedding theorem $||y||_C^2 \le h^{-1}||y||_{L_2}^2$ (e.g. [26]). In what follows we consider only one of the above two cases.

The discrete uniform (C) norms are defined in a standard manner

$$||v||_C = \max_{x\in\omega_h}|v(x)|, \quad |[v||_C = \max_{x\in\omega_h^-}|v(x)|, \omega_h^- = \omega_h \cup \{x_0 = 0\}, \tag{42}$$

and norm $||v]|_C$ is defined analogously to (42).

6.1. Estimate involving ψ_1

Our main result in this subsection is the following estimate:

$$-2\tau(\Delta v_{t\bar{x}}, \Delta v_{\bar{x}}^{(0.5)} + \psi_1^{(0.5)}] \le -(1 - 0.5\tau)||\Delta\hat{v}_{\bar{x}} + \hat{\psi}_1]|^2 + (1 + 0.5\tau)||\Delta v_{\bar{x}} + \psi_1]|^2 + \tau||(\psi_1)_t]|^2. \tag{43}$$

To prove (43), we multiply the first equation in (36) by $-2\tau\,\Delta v_{t\bar{x}}$ in the inner product sense (summing the respective terms from $i = 1$ to $i = N$). We analyse each term separately, starting with

$$-2\tau(\delta v_{t\bar{x}}, \Delta v_{\bar{x}}^{(0.5)}] = -||\Delta\hat{v}_{\bar{x}}]|^2 - ||\Delta v_{\bar{x}}||^2. \tag{44}$$

Then, by using

$$(fg)_t = f^{(0.5)} g_t + g^{(0.5)} f_t, \tag{45}$$

we transform the second term in the left hand side of (43). We sum the obtained two equalities up, and use a consequence of the so-called ϵ-inequality (e.g. [38])

$$|ab| \le \epsilon a^2 + \frac{1}{4\epsilon} b^2, \quad \epsilon > 0. \tag{46}$$

In particular, for $\epsilon = 0.5$ we have

$$\tau(\Delta\hat{v}_{\bar{x}} + \hat{\psi}_1, (\psi_1)_t] \le 0.5\tau||\Delta\hat{v}_{\bar{x}} + \hat{\psi}_1]|^2 + 0.5\tau||(\psi_1)_t]|^2, \tag{47}$$

with a similar expression for $\tau(\Delta v_{\bar{x}} + \psi_1, (\psi_1)_t]$. Note further that

$$||\Delta\epsilon_t||^2 \le \tfrac{1}{2}(||\Delta\hat{v}_x + \hat{\psi}_1||^2 + ||\Delta v_x + \psi_1||^2), \tag{48}$$

which follows immediately from the equation for the error of approximation

$$\Delta\epsilon_t = \Delta v_x^{(0.5)} + \psi_1^{(0.5)} \tag{49}$$

and the application of the ϵ-inequality (46). Combining these results leads immediately to (43).

6.2. Estimate involving ψ_2

Obtaining an estimate for the second equation in (36) is much more involved. The final result can be presented in the following form:

$$-2\tau\rho^{-1}(\Delta\epsilon_t, (\hat{\psi}_2)_{\bar{x}}) \ge -\tau c||\Delta\epsilon_t||^2 - \tau c||(\hat{\psi}_2)_{\bar{x}}||^2, \tag{50}$$

where c is a constant that does not dependent on grid steps τ and h, or approximate solution ϵ_h, $\bar{v}_h$, and θ_h, or the error of approximation $\Delta\epsilon_h$, $\Delta\bar{v}_h$, and $\Delta\theta_h$.

In what follows, we highlight key steps of obtaining this estimate. By using the second equation in (36), we obtain the following equality

$$-2\tau(\Delta\epsilon_t, \Delta v_{t\bar{x}}) = -2\tau\rho^{-1}\left(\Delta\epsilon_t, \left(\hat{l}_1\Delta\hat{\epsilon} + k_1(\hat{\epsilon}\Delta\hat{\theta} + \Delta\hat{\theta} + \Delta\hat{\theta}\Delta\hat{\epsilon}) + \sum_{k=2}^{5}\hat{l}_k\Delta\hat{\epsilon}^k\right)_{x\bar{x}} + (\hat{\psi}_2)_{\bar{x}}\right). \tag{51}$$

Then we analyse each term in (51). The technique used in the analysis requires additional identities and embedding theorems. In particular, we make use of the first Green's difference formula (see (25)):

$$(z, (ay_x)_{\bar{x}}) = [z_x, ay_x), \quad z_0 = z_N = 0, \quad a \equiv a(x), \quad x \in \omega_h, \tag{52}$$

the equality

$$\Delta\hat{\epsilon} = \Delta\epsilon^{(0.5)} + 0.5\tau\Delta\epsilon_t, \tag{53}$$

the Cauchy inequality (a direct consequence of the ϵ inequality (46)):

$$|(u, v)| \le ||u||||v|| \le \epsilon||u||^2 + \frac{1}{4\epsilon}||v||^2, \tag{54}$$

and the following embedding theorems

$$||u||^2 \le \frac{l^2}{8}||u_{\bar{x}}]|^2,\ u_0 = u_N = 0, \quad ||\Delta\theta||_C \le \frac{\sqrt{l}}{2}||\Delta\theta_{\bar{x}}]|,\ \theta_0 = \theta_N = 0,$$
$$||\Delta\theta_{\bar{x}}]| \le \frac{l}{2\sqrt{2}}||\Delta\theta_{\bar{x}x}||,\ \theta_0 = \theta_N = 0, \quad ||\Delta\theta|| \le \frac{l^2}{8}||\Delta\theta_{\bar{x}x}||. \tag{55}$$

Finally, we apply the following formulae for difference differentiation

$$(\Delta\hat{\epsilon}^k)_{\bar{x}} = \Delta\hat{\epsilon}_{\bar{x}}\sum_{m=0}^{k-1}\Delta\hat{\epsilon}^{k-1-m}\Delta\hat{\epsilon}^m_{(-1)}, \quad v_{(\pm1)} = v(x \pm h) = v_{i\pm1}, \tag{56}$$

$$(\Delta\epsilon^\alpha)_t = \Delta\epsilon_t\sum_{m=0}^{\alpha-1}\Delta\hat{\epsilon}^{\alpha-1-m}\Delta\epsilon^m \tag{57}$$

in order to arrive at (50).

6.3. Estimate involving ψ_3

The estimate for the error $\Delta\theta$,

$$\begin{aligned}2\tau(\Delta\theta_t\ &-\Delta\hat{\theta}_{\bar{x}x}, k_1(\hat{\theta}\Delta\hat{\epsilon}\Delta\epsilon_t + \hat{\epsilon}\Delta\hat{\theta}\Delta\epsilon_t + \epsilon_t\Delta\hat{\theta}\Delta\hat{\epsilon} + \Delta\hat{\theta}\Delta\hat{\epsilon}\Delta\epsilon_t) + \hat{\psi}_3) \le \tau c_v\epsilon_2||\Delta\theta_t||^2\\ &+ \tau k\epsilon_1||\Delta\hat{\theta}_{\bar{x}x}||^2 + \tau c(||\Delta\hat{\theta}||^2_C||\Delta\hat{\epsilon}||^2_C||\Delta\epsilon_t||^2_C + (||\Delta\hat{\epsilon}||^2_C + ||\Delta\hat{\theta}||^2_C)||\Delta\epsilon_t||^2\\ &+ ||\Delta\hat{\theta}||^2_C||\Delta\hat{\theta}_x||^2_1) + \tau c||\hat{\psi}_3||^2,\end{aligned} \tag{58}$$

is also obtained by using the technique described above. In (58) ϵ_i, $i = 1, 2$ are positive constants resulted from the application of the ϵ-inequality. A key point in obtaining (58) is the multiplication of (38) by $2\tau(\theta_t - \Delta\hat{\theta}_{\bar{x}x})$ in the scalar product sense.

6.4. Main energy inequality

In what follows, we use the following notation:

$$\begin{aligned} &l_0 = \text{const}, \quad l_1 = k_1(\theta - \theta_1) - 3k_2\epsilon^2 + 5k_3\epsilon^4 \geq l_0 > 0, \quad l_2 = -3k_2\epsilon + 10k_3\epsilon^3, \\ &l_3 = 10k_3\epsilon^2 - k_2, \quad l_4 = 5k_3\epsilon, \quad l_5 = k_3, \\ &l_1 + k_1\Delta\theta + \Phi_1^*(\Delta\epsilon) \geq \bar{l}_0 > 0, \end{aligned} \tag{59}$$

where

$$\Phi_1^*(\Delta\epsilon) = \sum_{k=1}^{4}\sum_{m=0}^{k} \Delta\epsilon_{(+1)}^{k-m}\Delta\epsilon^m l_{k+1}. \tag{60}$$

Then, summarising the results obtained in Sections 6.1–6.3, and using (48), we arrive at the following energy estimate for the error approximation obtained with scheme (34):

$$\begin{aligned} (1 - \tau c_1)||\hat{z}||_1^2 \; -\tau c \Bigg[&\left(||\Delta\hat{\theta}_x||_C^2 + \sum_{k=1}^{4} ||\Delta\hat{\epsilon}||_C^{2k} + ||\Delta\hat{\theta}||_C^2 \right) ||\Delta\hat{\epsilon}_x||_1^2 + (||\Delta\hat{\theta}||_C^2 + ||\Delta\hat{\theta}||_C^2||\Delta\hat{\epsilon}||_C^2 \\ &+ ||\Delta\hat{\epsilon}||_C^2)||\Delta\hat{v}_{\bar{x}} + \hat{\psi}_1]| \Bigg] + \tau c_v||\Delta\theta_t|| + \tau k||\Delta\hat{\theta}_{\bar{x}x}||^2 + I(z) \leq (1 + \tau c)||z||_1^2 \\ &+ \tau c(||\Delta\epsilon_x||_C^2 + f_1(\Delta\epsilon))||\Delta\epsilon_x||_1^2 + \tau c||\hat{\psi}||^2, \end{aligned} \tag{61}$$

where

$$\begin{aligned} I(z) = \; &\tau k(1 - (2\epsilon_1 + \epsilon_1||\Delta\hat{\epsilon}||_C^2))||\Delta\hat{\theta}_{\bar{x}x}||^2 + \tau^2\rho^{-1}[l_1 + k_1\Delta\hat{\theta} + \Phi_1^*(\Delta\hat{\epsilon}), \Delta\epsilon_{\bar{t}x}^2) \\ &+ \tau c_v(1 - 3\epsilon_2)||\Delta\theta_t||^2 + \tau^2(k + c_v)||\Delta\theta_{t\bar{x}}]|^2 \geq 0, \end{aligned} \tag{62}$$

$$f_1(\Delta\epsilon) = \left(1 + \sum_{k=1}^{3} ||\Delta\epsilon||_C^{2k} \right) ||\Delta\epsilon_x||_C^2 + \sum_{k=1}^{3} ||\Delta\epsilon||_C^k, \tag{63}$$

$$||\hat{\psi}||^2 = ||(\psi_1)_t]||^2 + ||(\hat{\psi}_2)_{\bar{x}}||^2 + ||(\hat{\psi}_3)||^2. \tag{64}$$

Norm $||\cdot||_1$ in (61),

$$||z||_1^2 = \rho^{-1}[l_1 + k_1\Delta\theta + \Phi_1^*(\Delta\epsilon), \Delta\epsilon_x^2) + ||\Delta v_{\bar{x}} + \psi_1]|^2 + (c_v + k)||\Delta\theta_{\bar{x}}]|^2, \tag{65}$$

is the norm used in the analysis of convergence in the case $\tau \leq h$. As we have already mentioned at the beginning of this section, condition $\tau \leq h$ is a consequence of the embedding theorem $||y||_C^2 \leq h^{-1}||y||_{L_2}^2$ connecting the uniform and L_2 discrete norms.

6.5. Convergence in the semi-norm W_2^1

Our procedure here follows the line of reasoning proposed originally in [27]. It is a two-stage procedure that has been applied to analyse convergence of difference schemes for nonlinear problems of mathematical physics. Recall that the ν-method cannot be applied in a straightforward manner to these problems [26]. Indeed, by estimating the error of the first difference derivative in the uniform metric, we would need to impose a restrictive condition like $\tau = h^\kappa$, $\kappa \geq 1$ which we would like to avoid. Hence, the idea here is to estimate first the difference derivative in the L_2 norm for $\tau \leq h$, and then to estimate it in the W_2^1 norm. By combining such two estimates we obtain an unconditional bound for the accuracy of the scheme in the uniform metric. Each case separately can be analysed with the ν-method. At the first step, it is straightforward to obtain a rough estimate of the error

$$||z_n||^2 \leq \nu^2(h^2 + \tau), \tag{66}$$

where the norm in (66) is defined as

$$||z||^2 = \rho^{-1}\bar{l}_0|[\Delta\epsilon_x||^2 + ||\Delta v_{\bar{x}}]|^2 + (c_v + k)||\Delta\theta_{\bar{x}}]|^2, \tag{67}$$

and $\bar{l}_0$ is defined as a constant that satisfies the following inequality: $l_1 + k_1\Delta\theta + \Phi_1^*(\Delta\epsilon) \geq \bar{l}_0 > 0$.

Then, we can derive an estimate for the error of the approximation at the $(n+1)$st time layer by considering a corresponding iterative process in a way similar to that described in [26]. A chain of recurrent relationships leads to the following estimate:

$$||z^{n+1}||^2 + \sum_{k=0}^{n} \tau(c_v||\Delta(\theta_t)_n||^2 + k||\Delta(\theta_{\bar{x}x})^{n+1}||^2) \leq f_1(\nu)(h^2 + \tau), \tag{68}$$

where $f_1(\nu)$ is a bounded function for sufficiently small step sizes τ and h. This estimate is then improved by using the main energy inequality (61). In particular, we obtain that

$$||\Delta\epsilon||_C, ||\Delta v||_C, ||\Delta\theta||_C \leq \nu_1(h^2 + \tau). \tag{69}$$

At the second step of our procedure, we analyse convergence of our difference scheme in the discrete norm W_2^1. This is done for the case of $\tau \geq h$ and hence the embedding theorems (55) are in use. Similarly to the above, we obtain that

$$||\Delta\epsilon_x||_C, ||\Delta\theta_x||_C \leq \nu_2(h^2 + \tau). \tag{70}$$

The norm used for this analysis is

$$||z||_2^2 = \rho^{-1}[l_1 + k_1\Delta\theta, \Delta\epsilon_x^2) + ||\Delta v_{\bar{x}} + \psi_1]|^2 + (c_v + k)||\Delta\theta_{\bar{x}}]|^2. \tag{71}$$

Finally, the convergence in the semi-norm W_2^1 is obtained as a result of the combination of the above two results by choosing as ν the maximum of the two values of ν_1 and ν_2:

$$\{||\Delta\epsilon_{\bar{x}}]|^2 + ||\Delta v_{\bar{x}}]|^2\} + ||\Delta\theta_{\bar{x}}]|^2 + \sum_{t\in\omega_\tau} \tau||\Delta\theta_t||^2 + \sum_{t\in\omega_\tau} \tau||\Delta\hat{\theta}_{\bar{x}x}||^2\}^{1/2} \leq \nu(h^2 + \tau). \tag{72}$$

7. Numerical experiments

The scheme described and analysed in Sections 4–6 has been applied to modelling the dynamics of shape memory alloy materials. The major goal of the computational experiments reported below is to demonstrate that the scheme is capable of efficiently quantifying phase transformations and associated hysteresis phenomena in materials with shape memory. As an example, we consider a $Au_{23}Cu_{30}Zn_{47}$ rod of length $L = 1$ cm. Physical parameters for this material are available in the literature [14,31,33] and in the context of system (8) we have

$$k = 1.9 \times 10^{-2}\,\mathrm{cm\,g/(ms^3\,K)}, \quad \rho = 11.1\,\mathrm{g/cm^3}, \quad \theta_1 = 208\,\mathrm{K}, \quad k_1 = 480\,\mathrm{g/(ms^2\,cm\,K)},$$
$$k_2 = 6 \times 10^6\,\mathrm{g/(ms^2\,cm\,K)}, \quad C_v = 29\,\mathrm{g/(ms^2\,cm\,K)}, \quad k_3 = 4.5 \times 10^8\,\mathrm{g/(ms^2\,cm\,K)},$$

where ms in the above units stands for milli-seconds. We analyse the behaviour of the $Au_{23}Cu_{30}Zn_{47}$ rod under different time-varying distributed mechanical loadings.

One of the advantages of fully conservative schemes lies with the fact that they can be used effectively on coarse grids. Indeed, all results reported below have also been performed with $N = 24$. Our iterative process for solving (15)–(19) is based on Newton's iterations with a Jacobian-based preconditioner.

A Ginzburg capillarity effect has been formally included in the implemented model. However, since the Ginzburg coefficient reported in the literature is typically small, we neglect this effect in the present computations.

We start our computational analysis with the low temperature case, where one would expect a well pronounced hysteresis effects. The implementation of the scheme has been carried out in (ϵ, v, θ) variables. The boundary conditions for the problem have been taken as $v = 0, \epsilon_x = 0$ (e.g. [9]) with zero heat fluxes $(\partial\theta/\partial x = 0)$. No thermal loading was assumed $(G = 0)$. The initial conditions for this first experiment have been taken as follows:

$$\theta^0 = 220, \quad u^0 = \begin{cases} 0.11869x, & 0 \le x \le 0.25, \\ 0.11869(0.5 - x), & 0.25 \le x \le 0.75, \\ 0.11869(x - 1), & 0.75 \le x \le 1, \end{cases} \quad v^0 \equiv u^1 = 0. \tag{73}$$

The time-varying mechanical loading in this experiment has been defined by (see Fig. 1, lower left plot)

$$F = 7000\,\sin^3\left(\tfrac{1}{2}\pi t\right), \tag{74}$$

given in the $\mathrm{g/(ms^2\,cm^2)}$ units (that is the load/stress per unit length). In the upper plots of Fig. 1 we present both displacement and strain as functions of space and time. In this case, the material behaves like a "quasiplastic" sample (see, e.g. [32]) and a wide hysteresis loop is an intrinsic feature of the process. This is demonstrated by the lower right plot in Fig. 1. This plot has been obtained for a fixed spatial grid point (taken in all experiments as $n_h = n/2 - 3$) by plotting the displacement u as a function of F.

Having succeeded in reproducing the hysteretic behaviour of a SMA rod under low temperature conditions, our next goal has been to analyse the behaviour of the sample under an increased initial temperature.

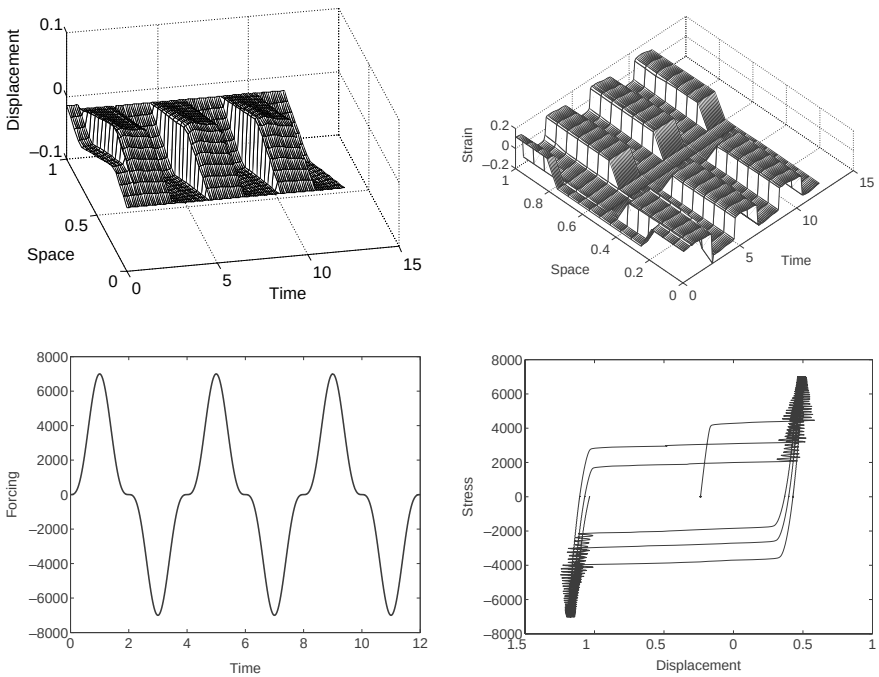

Fig. 1. Mechanically induced phase transformations and associated hysteresis effects in a SMA rod.

We have observed not only quantitatively, but qualitatively different behaviour. We have changed the time-varying mechanical loading to a sharp profile, defining it now by

$$F = 7000 \begin{cases} \frac{1}{3}t, & 0 \le t \le 3, \\ \frac{1}{3}(6-t), & 3 \le t \le 9, \\ \frac{1}{3}(t-12), & 9 \le t \le 12, \end{cases} \tag{75}$$

and looked at the spatio-temporal distribution of strain. For the low temperature case, the qualitative behaviour of the sample remains the same as the one depicted in the upper right plot of Fig. 1. The

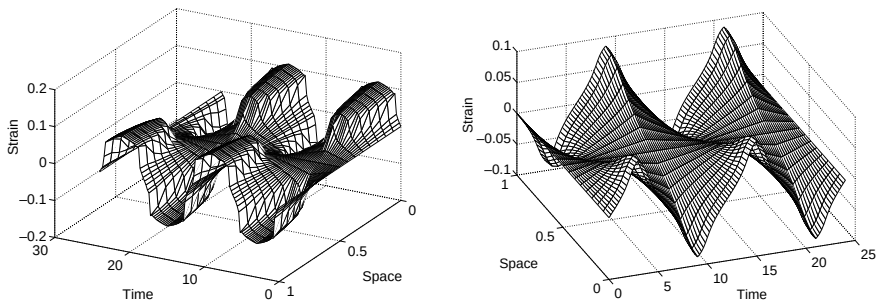

Fig. 2. Spatio-temporal strain distributions for the medium ($T = 260^\circ$, left) and high ($T = 310^\circ$, right) temperature regimes.

increased temperature produces a qualitatively different behaviour. In the medium temperature range, the sample is expected to be in the "pseudoelastic" regime, while under the high temperature regime the sample attains features of an "almost elastic" rod (see, e.g. [32]). The strain distributions in these two cases (for $\theta^0 = 260$ and $\theta^0 = 310$, respectively) are shown in Fig. 2.

Next, we have analysed displacements as a function of space-time and as a function of loading in a systematic manner. In particular, we have taken the same sample with the same initial and boundary conditions as above with the mechanical time-varying loading (75). We have been changing initial temperature values of the sample in a range between 220 and 310 °K and observe the behaviour of the SMA rod under

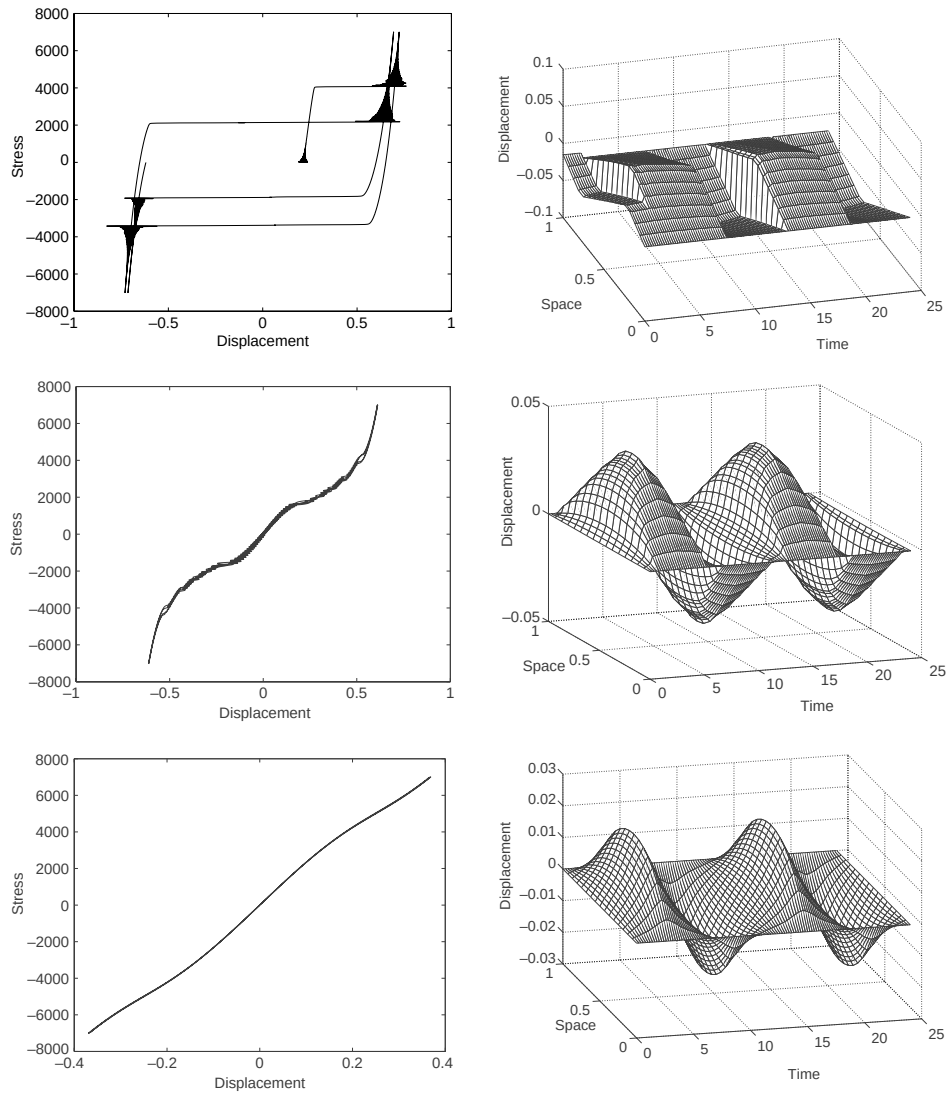

Fig. 3. Mechanically induced hysteresis for low ($T = 220°$, upper plot), medium ($T = 260°$, middle plot), and high ($T = 310°$, lower plot) temperature regimes (left: hysteresis characterisations; right: mechanical displacements).

the mechanical loading given in form (75). As before, a wide hysteresis loop is clearly pronounced in the low temperature regime (see upper plots in Fig. 3). This regime has its analogy in quasiplastic materials. Note also that for shape memory alloy materials this regime corresponds to the situation where the free energy function has two pronounced minima that correspond to the martensitic variants (twins) in our case. As seen from Fig. 3, the stress–strain dependency varies substantially over the temperature range of operation, exhibiting strongly nonlinear behaviour.

Then, we have increased the temperature to the medium range of values. We have observed a fundamentally different behaviour of the SMA sample. Two small symmetric hysteresis loops are formed in this case and the profile of displacement becomes smoother as compared to the "quasiplastic" case. This situation, typical for "pseudoelastic" materials, is presented in the middle plots of Fig. 3. From a physical point of view, this corresponds to the situation where all three phases considered with our model (one austenite and two twin martensite) may coexist (e.g. [32]). In this case, the free energy function has three minima that correspond to our possible equilibrium configurations.

Finally, we have moved the sample to the high temperature phase by increasing the initial temperature to 310 °K. As demonstrated by the lower plots in Fig. 3, hysteresis effects are practically absent in this case. The free energy function has a single minimum that corresponds to the (austenite) equilibrium configuration. Nonlinearities are small and the sample is in an "almost elastic" regime.

8. Conclusions

In this paper, we applied a new conservative difference scheme to the analysis of behaviour of materials with shape memory. Firstly, we noted that the general system of 2D PDEs describing a coupled strongly nonlinear behaviour of a thermomechanical physical system with shape memory effects can be reduced to the 1D Falk model in a number of practically interesting cases. Then, we presented a new fully conservative implicit scheme for solving the problem. We underlined a general procedure for the analysis of the scheme and highlighted the main steps leading to unconditional convergence of the proposed numerical approximation. Finally, the constructed and analysed scheme was applied to the investigation of the behaviour of a shape memory alloy rod under different physically plausible conditions. In particular, we demonstrated that the proposed scheme can reproduce effectively, even on coarse grids, the entire range of SMA sample behaviour, from quasiplastic, to pseudoelastic, and to almost elastic cases. Strong nonlinearities, including hysteresis effects, were analysed with several numerical examples.

References

[1] R. Abgrall, Towards the ultimate conservative scheme: following the quest, J. Comput. Phys. 167 (2001) 277–315.
[2] V.N. Abrashin, Difference schemes for nonlinear hyperbolic equations, Differ. Equations 11 (1975) 294–303.
[3] V.N. Abrashin, Stable difference schemes for quasilinear equations of mathematical physics, Differ. Equations 18 (1982) 1967–1971.
[4] V.N. Abrashin, A class of finite difference schemes for nonstationary nonlinear problems of mathematical physics, Differ. Equations 22 (1986) 759–769.
[5] M. Amara, D. Capatina-Papaghiuc, A. Chatti, New locking-free mixed method for the Reissner-Mindlin thin plate model, SIAM J. Numer. Anal. 40 (2002) 1561–1582.
[6] F. Auricchio, E. Sacco, Thermo-mechanical modelling of a superelastic shape memory wire under cyclic stretching-bending loadings, Int. J. Solid Struct. 38 (2001) 6123–6145.

[7] J.M. Ball, et al., On the dynamics of fine structure, J. Nonlinear Sci. 1 (1991) 17–70.
[8] A.Y. Boiko, The construction of completely conservative difference schemes by algorithms of the projection method, Comput. Math. Math. Phys. 27 (1987) 147–155.
[9] N. Bubner, Landau-Ginzburg model for a deformation-driven experiment on shape memory alloys, Continuum Mech. Thermodyn. 8 (1986) 293–308.
[10] N. Bubner, G. Mackin, R.C. Rogers, Rate dependence of hysteresis in one-dimensional phase transitions, Comput. Mater. Sci. 18 (2000) 245–254.
[11] R. Courant, K.O. Friedrichs, H. Lewy, Uber die partiellen differenzengleichungen der mathematischen physik, Math. Ann. 100 (1928) 32–74.
[12] V. Dorodnitsyn, Noether-type theorems for difference equations, Appl. Numer. Math. 39 (2001) 307–321.
[13] N.O. Dzhgamadze, A.V. Popov, The convergence of a difference scheme for the 2D equations of gas dynamics, Comput. Math. Math. Phys. 32 (1992) 521–529.
[14] F. Falk, Model free energy, mechanics, and thermomechanics of shape memory alloys, Acta Metall. 28 (1980) 1773–1780.
[15] D. Furihata, Finite difference schemes for $\partial u/\partial t = (\partial/\partial x)^{\alpha}\delta G/\delta u$ that inherit energy conservation or dissipation property, J. Comput. Phys. 156 (1999) 181–205.
[16] D. Furihata, A stable and conservative finite difference scheme for the Cahn-Hilliard equation, Numer. Math. 87 (2001) 675–699.
[17] V.M. Goloviznin, A.A. Samarskii, A.P. Favorskii, Variational Approach to Construction of finite-difference mathematical models in hydrodynamics, Dokl. USSR Acad. Sci. 235 (1977) 1285–1288.
[18] V.M. Goloviznin, et al., Fully conservative correction of fluxes in the problems of gasdynamics, Dokl. USSR Acad. Sci. 274 (1984) 524–528.
[19] F.E. Ham, F.S. Lien, A.B. Strong, A fully conservative second-order finite difference scheme for incompressible flow on nonuniform grids, J. Comput. Phys. 177 (2002) 117–133.
[20] T. Ichitsubo, et al., Kinetics of cubic to tetragonal transformation under external field by the time-dependent Ginzburg–Landau approach, Phys. Rev. B 62 (2000) 5435–5441.
[21] A.E. Jacobs, Landau theory of structures in tetragonal-orthorhombic ferroelastics, Phys. Rev. B 61 (2000) 6587–6595.
[22] T. Kerkhoven, On the 1D current driven semiconductor equations, SIAM J. Appl. Math. 51 (1991) 748–774.
[23] V.A. Korobitsyn, Invariant variational-difference schemes and conservation laws, Comput. Math. Math. Phys. 29 (1989) 71–79.
[24] S.Y. Leu, Limit analysis of viscoplastic flows using an extended general algorithm sequentially: convergence analysis and validation, Comput. Mech. 30 (2003) 421–427.
[25] T. Matsuo, et al., Spatially accurate dissipative or conservative finite difference schemes derived by the discrete variational method, Jpn. J. Indust. Appl. Math. 19 (2002) 311–330.
[26] P.P. Matus, On unconditional convergence of difference schemes for gas dynamics problems, Differ. Equations 21 (1985) 1227–1238.
[27] P.P. Matus, L.V. Stanishevskaya, Unconditional convergence of difference schemes for nonstationary quasilinear equations of mathematical physics, Differ. Equations 27 (1991) 1203–1219.
[28] P.P. Matus, M.N. Moskalkov, V.S. Scheglik, Consistent estimate of the convergence rate for the grid method in the case of a second-order nonlinear equation with generalized solution, Differ. Equations 31 (1995) 1249–1256.
[29] P. Matus, R.V.N. Melnik, I.V. Rybak, Fully Conservative Difference Schemes for Nonlinear Models Describing Dynamics of Materials with Shape Memory, Dokl. Acad. Sci. Belarus 47 (2003) 15–18.
[30] R.V.N. Melnik, A.J. Roberts, K.A. Thomas, Computing dynamics of copper-based SMA via centre manifold reduction of 3D models, Comput. Mater. Sci. 18 (2000) 255–268.
[31] R.V.N. Melnik, A.J. Roberts, K.A. Thomas, Coupled thermomechanical dynamics of phase transitions in shape memory alloys and related hysteresis phenomena, Mech. Res. Commun. 18 (2001) 637–651.
[32] R.V.N. Melnik, A.J. Roberts, K.A. Thomas, Phase transitions in shape memory alloys with hyperbolic heat conduction and differential–algebraic models, Comput. Mech. 29 (2002) 16–26.
[33] M. Niezgodka, J. Sprekels, Convergent numerical approximations of the thermomechanical phase transitions in shape memory alloys, Numer. Math. 58 (1991) 759–778.
[34] V.V. Ostapenko, Equivalent definitions of conservative finite-difference schemes, Comput. Math. Math. Phys. 29 (1989) 100–110.

[35] I. Pawlow, Three dimensional model of thermomechanical evolution of shape memory materials, Control Cybern. 29 (2000) 341–365.
[36] Y.P. Popov, A.A. Samarskii, Fully conservative difference schemes for equations of magneto-hydrodynamics, Comput. Math. Math. Phys. 10 (1970) 990–998.
[37] I.F. Potapenko, C.A. de Azevedo, The completely conservative difference schemes for the nonlinear Landau–Fokker–Planck equation, J. Comput. Appl. Math. 103 (1999) 115–123.
[38] A.A. Samarskii, The Theory of Difference Schemes, Marcel Dekker, NY, 2001.
[39] A.N. Tichnov, A.A. Samarskii, Convergence of difference schemes in the class of discontinuous coefficients, Dokl. Acad. Sci. USSR 124 (1959) 529–532.
[40] V.F. Tishkin, Variational difference schemes for the dynamic equations of deformable media, Differ. Equations 21 (1985) 865–870.
[41] L.G. Volkov, The construction of completely conservative difference schemes for the equations of the nonlinear theory of elasticity, Comput. Math. Math. Phys. 31 (1991) 92–99.
[42] L. Wang, R.V.N. Melnik, Nonlinear coupled thermomechanical waves modelling shear type phase transformation in shape memory alloys, in: G.C. Cohen et al. (Eds.), Mathematical and Numerical Aspects of Wave Propagation, Springer, 2003, pp. 723–728.